

Endovascular ascending aortic pseudoaneurysm repair under image fusion guidance and transcranial Doppler monitoring

Lauren A. Fitzgerald, BS,^{a,b} Lamees I. El Nihum, BS,^{a,b} Pauline M. Berens, BS, BA,^c Ponraj Chinnadurai, MBBS, MMST,^{b,d} Zsolt Garami, MD,^b and Marvin D. Atkins, MD,^b *Bryan and Houston, TX; and Malvern, PA*

ABSTRACT

We describe a 78-year-old woman with a large ascending aortic pseudoaneurysm who underwent thoracic endovascular aortic repair under intraoperative image fusion guidance and real-time transcranial Doppler (TCD) monitoring. TCD monitoring revealed a total of 419 microembolic signals throughout the procedure, with the majority occurring as the first stent graft crossed the ascending aorta. Two days later, she underwent endovascular repair of a graft type IA endoleak. We highlight the role of image fusion guidance and TCD monitoring in enabling successful thoracic endovascular aortic repair in an elderly woman and in identifying procedural areas of improvement to minimize stroke risk. (*J Vasc Surg Cases Innov Tech* 2022;8:425-8.)

Keywords: TEVAR; Transcranial Doppler; Image fusion

Intraoperative transcranial Doppler (TCD) monitoring during thoracic endovascular aortic repair (TEVAR) is an appropriate layer of protection to mitigate risk of embolization in elderly patients with multiple comorbidities, allowing high-risk patients to be candidates for endovascular repair despite high stroke risk. We describe a 78-year-old woman who underwent successful TEVAR for an ascending aortic aneurysm under intraoperative image fusion guidance and real-time TCD monitoring.

CASE REPORT

A 78-year-old woman with early stage pancreatic cancer presented for routine imaging, which revealed a large ascending aortic pseudoaneurysm. She was transferred to the emergency department with new onset of severe, mid-sternal chest pain. Contrast-enhanced computed tomography angiography (CTA) demonstrated a large saccular pseudoaneurysm in the proximal anterior ascending aorta. The enhancing saccular component was approximately 4.1 × 2.6 × 3.6-cm with an eccentric

thrombus and a 1.5-cm neck. A second 4.1-cm saccular aneurysm was present in the ascending aorta. The etiology was likely her multiple atherosclerotic plaques leading to penetrating ulcers with evolution into pseudoaneurysms. She was not a candidate for open surgical repair owing to her advanced age, frailty, and multiple comorbidities. The decision was made to proceed with TEVAR with TCD monitoring. As the distance from the highest coronary ostium to the brachiocephalic artery (BCA) ostium was less than 7 cm, we elected to place cuffs rather than a thoracic stent graft to preserve both ostia. The shortened delivery sheath of the aortic stent graft (cuff) necessitated delivery of the endoprosthesis through upper extremity rather than femoral access. The authors attest they are in compliance with human studies committees and animal welfare regulations of the authors' institutions and Food and Drug Administration guidelines, including patient consent where appropriate.

Before the procedure, the right middle cerebral artery (MCA) was insolated with color flow, pulsed-wave TCD to monitor the temporal lobe of the brain. A temporary pacemaker was placed via a 7F right internal jugular introducer under fluoroscopic guidance in the right ventricle for rapid ventricular pacing at 180 bpm to mitigate distal migration of the graft during deployment. A 5F sheath was inserted in the femoral artery, and a pigtail catheter was advanced to at the level of the aortic annulus. An incision was made in the deltopectoral groove and the right axillary artery was exposed. A 6F sheath was introduced through the right axillary artery using standard Seldinger technique; this was later upsized to an 18F sheath (Core DrySeal, W. L. Gore & Associates, Inc., Flagstaff, AZ). A Bentson wire (Cook Medical, Bloomington, IN) was placed through the ascending aorta, aortic valve, and into the left ventricle. The Bentson wire was exchanged for a double curved Lunderquist wire (Cook Medical) via an angled pigtail catheter.

Preoperative CTA images were imported in a three-dimensional (3D) postprocessing workstation and key vascular

From the Texas A&M College of Medicine, Bryan, TX^a; DeBakey Heart & Vascular Center, Houston Methodist Hospital, Houston, TX^b; Baylor College of Medicine, Houston, TX^c; and Advanced Therapies, Siemens Medical Solutions USA, Inc., Malvern.^d

Author conflicts of interest: P.C. is a full-time employee and Senior Key Expert at Advanced Therapies Division, Siemens Medical Solutions USA, Inc., Malvern, PA. All other authors do have no conflicts of interest to disclose.

Correspondence: Marvin D. Atkins, MD, Houston Methodist DeBakey Heart & Vascular Center, 6550 Fannin St, Smith Tower Ste 1401, Houston, Texas 77030 (e-mail: mdatkins@houstonmethodist.org).

The editors and reviewers of this article have no relevant financial relationships to disclose per the Journal policy that requires reviewers to decline review of any manuscript for which they may have a conflict of interest.

2468-4287

© 2022 The Author(s). Published by Elsevier Inc. on behalf of Society for Vascular Surgery. This is an open access article under the CC BY-NC-ND license (<http://creativecommons.org/licenses/by-nc-nd/4.0/>).

<https://doi.org/10.1016/j.jvscit.2022.06.009>

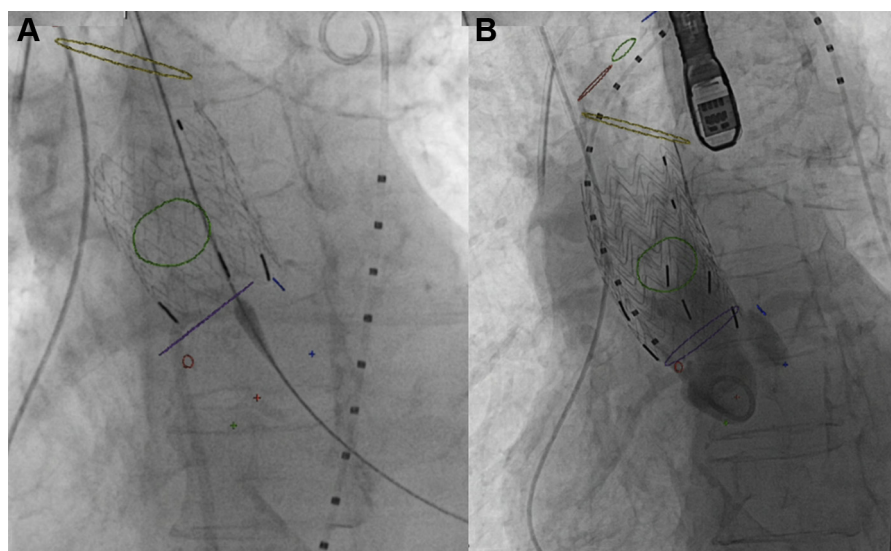


Fig 1. Aortic stent graft deployment. Live fluoroscopic image showing deployment of first **(A)** and second **(B)** aortic stent graft (cuff) in the ascending aorta using computed tomography (CT) image fusion markers. Image fusion markers: blue circle = left coronary artery ostium; blue dot = nadir of left coronary sinus; green circle = ostium of ascending aortic pseudoaneurysm; green dot = nadir of noncoronary sinus; purple circle (shown as a line) = sinotubular junction (STJ); red circle = right coronary artery (RCA) ostium; red dot = nadir of right coronary sinus; yellow circle = proximal origin of right brachiocephalic artery (BCA). Supra-aortic vessels: red circle = right BCA; green circle = left common carotid artery; blue circle = left subclavian artery.

landmarks were electronically annotated. Optimal deployment angle for the stent graft that aligned the sinotubular junction (STJ), right coronary artery (RCA) ostium and right BCA ostium was derived at LAO21 and CRAN 3. CT images were then fused with intraoperative two-dimensional fluoroscopy using 3D-3D image fusion technique after acquiring 4-second noncontrast cone beam CT images (DynaCT (Siemens Healthineers, Erlangen, Germany)). After image fusion, vascular landmarks from pre-operative CTA were overlaid on two-dimensional fluoroscopy to guide deployment of the stent graft in relation to the STJ and RCA ostium proximally and the right BCA ostium distally.

A 36 × 36 × 45-mm Gore Excluder AAA endoprosthesis (W. L. Gore & Associates, Inc.) was advanced to the STJ and deployed using angiography to confirm proper placement, covering the origin of the pseudoaneurysm without interfering with the RCA ostium (Fig 1, A). A second a 36 × 36 × 45-mm Gore Excluder AAA endoprosthesis was then deployed with 50% overlap just below the right BCA (Fig 1, B). Completion angiography revealed good flow in the coronary arteries and no flow in the pseudoaneurysm.

TCD monitoring was performed throughout the procedure. Doppler parameters for our PMD100 (Spencer Technologies, Medway, MA) were: transducer, 2-MHz; circular probe surface, 13 mm; pulse repetition frequency, 8 kHz; fast Fourier transformation, 128 points; overlap, 66%; sample volume axial length, 6 mm; output power, 100% [700-mW/cm² spatial peak temporal average intensity]; filter, 125 Hz; range, 30 dB; Doppler volume 4 dB, M-mode range, 30 dB; and sweep period, 4 seconds. TCD monitoring revealed a total of 419 microembolic signals (MES) throughout the entire procedure, with 107

occurring during the wire exchange, pigtail maneuvering, and contrast administration, 110 as the first stent graft crossed the ascending aorta (Fig 2, A), 70 during the first stent graft deployment (Fig 2, B), 40 as the second graft crossed the ascending aorta (Fig 2, C), and 67 during the second graft deployment (Fig 2, D). No cerebral malperfusion was noted.

Two days after graft placement, the patient demonstrated a type IA endoleak of the ascending aortic graft on electrocardiogram-gated CTA images, although no residual endoleak was appreciated by angiography on initial deployment (Fig 3). The patient returned to the hybrid operating room.

The endoleak was repaired with an additional 36 × 36 × 45-mm Gore Excluder AAA endoprosthesis more proximally, extending to the level of the STJ. This was augmented with balloon angioplasty of the stent graft with a Gore Tri-Lobe Balloon (W. L. Gore & Associates). No flow was noted in the pseudoaneurysm at case end.

The patient was discharged 2 days later. Outpatient electrocardiogram-gated CT 1 month later showed minimal, stable type IA endoleak at the proximal landing zone. No intervention was performed given marked improvement of contrast opacification and flow within the pseudoaneurysm. She was scheduled for continued follow-up.

DISCUSSION

Ascending aortic pathologies are treated with conventional open surgery with median sternotomy and cardiopulmonary bypass, often requiring circulatory arrest and deep hypothermia.¹⁻³ Recently, the feasibility of TEVAR for ascending aortic pathologies has been

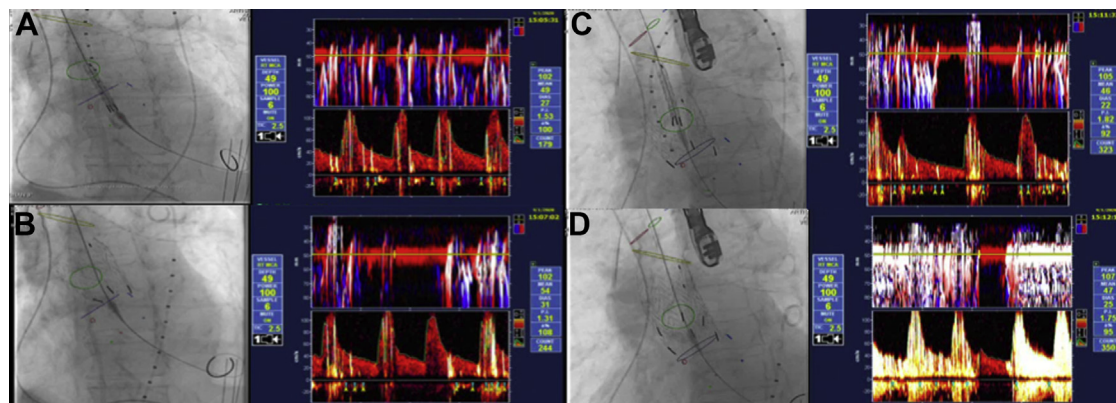


Fig 2. Live fluoroscopy and corresponding intraoperative transcranial Doppler monitoring image demonstrating microemboli during various stages of deployment of ascending aortic stent graft. Transcranial Doppler monitoring revealed a total of 419 microembolic signals (MES) throughout the entire procedure, with 107 occurring during the wire exchange, pigtail maneuvering and contrast administration; 110 as the first stent graft crossed the ascending aorta (**A**); 70 during the first stent graft deployment (**B**); 40 as the second graft crossed the ascending aorta (**C**); and 67 during the second graft deployment (**D**).

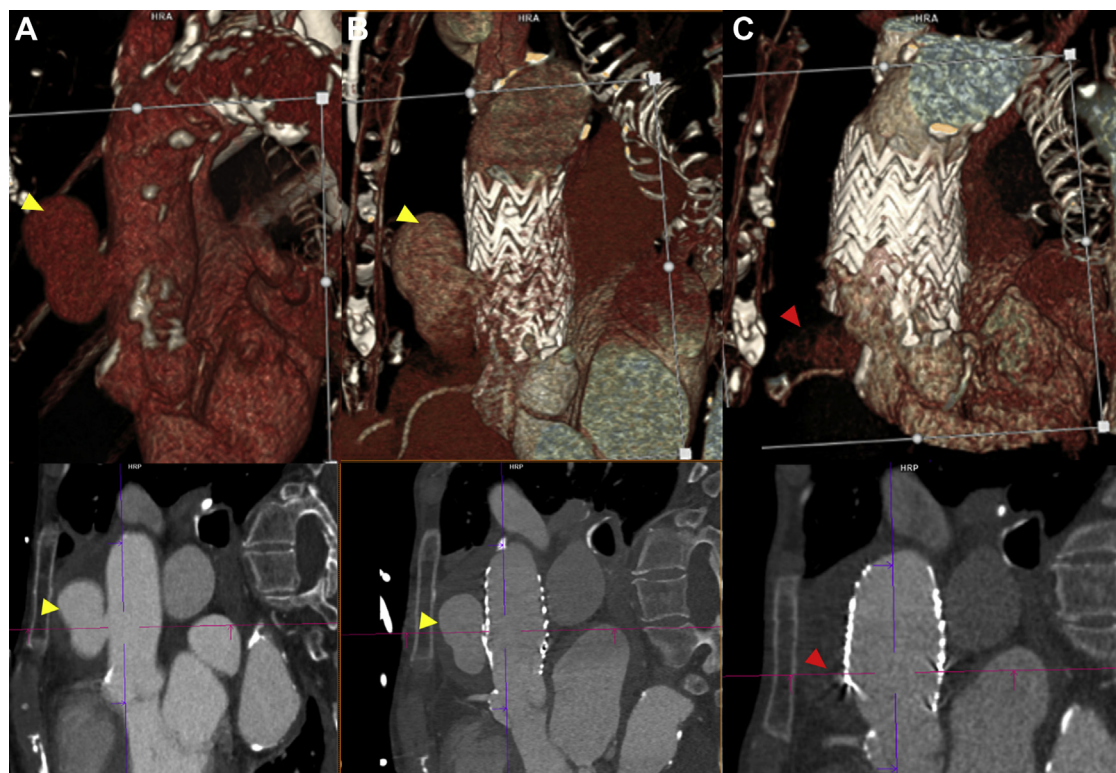


Fig 3. Type IA endoleak after graft deployment. Computed tomography angiography (CTA) (oblique sagittal and volume-rendered views) showing ascending aortic pseudoaneurysm (yellow arrow) before aortic stent graft placement (**A**) and after aortic stent graft placement (**B**). After ballooning and additional stent graft deployment (**C**), a type IA endoleak (red arrow) of the ascending aortic graft after graft deployment was noted, although no residual endoleak was appreciated initially by angiography.

demonstrated in high-risk surgical candidates using devices originally designed for the descending or abdominal aorta, potentially increasing risk of embolization owing in part to the off-label nature of graft use.^{3,4} We present the use of TCD monitoring during TEVAR to

assess cerebral perfusion and mitigate risks of embolization in our patient.

MES during cardiovascular operations have been linked to postoperative cognitive decline and decreased quality of life.⁵ Stroke occurs in 3% to 8% of patients undergoing

TEVAR, with the highest incidence during thoracic aortic aneurysm repair.^{6,7} Patients with approximately 50 MES on TCD intraoperatively have increased stroke risk.⁷ Additionally, silent cerebral infarction is believed to occur in more than 60% of TEVAR.⁶

Benson et al⁵ indicated that pigtail and guidewire insertion and maneuvering seemed to carry the highest intraoperative risk of MES on TCD during TEVAR. However, our case revealed that the majority of MES (n = 110) occurred as the first stent graft crossed the ascending aorta, whereas MES during wire exchange, pigtail maneuvering, and contrast administration was a close second (n = 107). Future studies may further characterize which technical aspects of these procedures carry a higher risk of MES, thus pointing out opportunities for improved or innovative procedural technique.

Finally, TCD allows for the identification of cerebral malperfusion. If the TCD signal remains constant in the presence of microemboli, this observation would indicate asymptomatic microemboli and that the MCA is not occluded. If the TCD signal changes, however, this observation would indicate MCA occlusion and necessitate mitigation via immediate transfer of the patient to the neurointerventional suite for clot retrieval.

CONCLUSIONS

TEVAR under image fusion guidance and real-time TCD monitoring enabled successful repair of an

ascending aortic aneurysm in an elderly woman. TCD monitoring during TEVAR may mitigate the risk of embolization in patients and provide direction in identifying procedural areas of improvement to minimize stroke risk.

REFERENCES

1. Qureshi MI, Davies AH. Endovascular aneurysm repair in the elderly: first do no harm. *Vascular* 2018;26:113-4.
2. Baikoussis NC, Antonopoulos CN, Papakonstantinou NA, Argiriou M, Geroulakos G. Endovascular stent grafting for ascending aorta diseases. *J Vasc Surg* 2017;66:1587-601.
3. Piffaretti G, Grassi V, Lomazzi C, Brinkman WT, Navarro TP, Jenkins MP, et al; GREAT participants. Thoracic endovascular stent graft repair for ascending aortic diseases. *J Vasc Surg* 2019;70:1384-9.e1.
4. Doblar DD. Intraoperative transcranial ultrasonic monitoring for cardiac and vascular surgery. *Semin Cardiothorac Vasc Anesth* 2004;8:127-45.
5. Benson RA, Matthews D, Loftus V, Nicholson G, Tropman D, Loftus IM. Cerebral embolization during endovascular infrarenal, juxtarenal, and suprarenal aortic aneurysm repair, high-risk maneuvers, and associated neurologic outcomes. *J Vasc Surg* 2018;68:1374-81.
6. Grover G, Perera AH, Hamady M, Rudarakanchana N, Barras CD, Singh A, et al. Cerebral embolic protection in thoracic endovascular aortic repair. *J Vasc Surg* 2018;68:1656-66.
7. Bismuth J, Garami Z, Anaya-Ayala JE, Naoum JJ, El Sayed HF, Peden EK, et al. Transcranial Doppler findings during thoracic endovascular aortic repair. *J Vasc Surg* 2011;54:364-9.

Submitted Feb 20, 2022; accepted Jun 19, 2022.